LWT - Food Science and Technology 71 (2016) 88–95

Contents lists available at ScienceDirect

LWT - Food Science and Technology

journal homepage: www.elsevier.com/locate/lwt

Effect of TiO_2 nanoparticles on the physico-mechanical and ultraviolet light barrier properties of fish gelatin/agar bilayer film

Akbar Vejdan [a], Seyed Mahdi Ojagh [a, **], Afshin Adeli [a], Mehdi Abdollahi [b, *]

[a] Department of Fisheries, Gorgan University of Agricultural Sciences and Natural Resources, Gorgan, Iran
[b] Department of Seafood Science and Technology, Faculty of Marine Sciences, Tarbiat Modares University, P.O. Box 46414-356, Noor, Iran

ARTICLE INFO

Article history:
Received 15 November 2015
Received in revised form
6 March 2016
Accepted 7 March 2016
Available online 10 March 2016

Keywords:
Agar
Fish gelatin
Nanocomposite
Bilayer film
Titanium dioxide

ABSTRACT

Bilayer gelatin/agar films containing different concentrations of TiO_2 (0.5, 1, and 2 g/100 g) were prepared by incorporation of anatase titanium dioxide nanoparticles in the fish gelatin layer of the bilayers. Gelatin/agar bilayer film was produced from the monolayers using the casting method in two steps and their microstructural, physical, mechanical and optical characteristics were studied. Results showed that the addition of TiO_2 decreased water vapor permeability of the bilayers more than 30%, upon increasing TiO_2 content to 2 (g/100 g). However, swelling ratio and moisture content increased with the increase in the nano-TiO_2 content, probably due to the hydrophilic nature of the TiO_2 nanoparticles. The tensile strength of the bilayer films increased from 10.80 to 13.91 MPa upon increasing nano-TiO_2 content from 0 to 0.5 (g/100 g); however, tensile strength decreased with further increase of the nanoparticle concentration. In addition, the metallic nature of nano-TiO_2 considerably improved the barrier properties of the bilayer films against UV light at low concentration, while it increased their opacity. This property might help in the preservation of light-sensitive foods, but more studies on real food systems are required.

1. Introduction

Increasing environmental problems with petrochemical-based plastic packaging have caused a rising inclination to use biodegradable packaging materials from natural polymers (Weber, Haugaard, Festersen, & Bertelsen, 2002). Among these proteins, gelatin is considered a good candidate for food packaging because it is inexpensive and has good film-forming capability, as well as high availability and biodegradability (Farris et al., 2011).

Gelatin is obtained from the skins and bones of bovine, porcine and fish wastes. Recently, the use of fish gelatin, given the increasing risk of transmitting pathogens like bovine spongiform encephalopathy, has increased (Kim & Mendis, 2006a, 2006b). However, studies have shown that fish gelatin films are brittle (Yakimets et al., 2005), and their hydrophilic nature connotes high water solubility and water vapor permeability. Different strategies have been suggested to overcome these weaknesses, including chemical modification and adding crosslinking agents (Martucci & Ruseckaite, 2009), adding nanoparticles (Kanmani & Rhim, 2014) and developing film blends and bilayers with polysaccharides (Rhim & Wang, 2013).

In this regard, agar is a polysaccharide extracted from marine red algae, which is biocompatible, has high mechanical strength and possesses good film-forming properties (Freile-Pelegrín et al., 2007). Agar is relatively insoluble in water and its films possess good water resistance. This polysaccharide has the ability to produce strong gels which can help to reduce the water vapor permeability of films (Pavlath, Gosset, Camirand, & Roberton, 1999).

Preventing food spoilage from light-induced oxidation is one of the greatest concerns in the food industry (Li et al., 2011). Despite having good mechanical and relatively good oxygen barriers properties (Martucci & Ruseckaite, 2009), protein- or polysaccharide-based films do not have adequate barrier properties against UV light (Ramos et al., 2013) and cannot properly prevent the photooxidation of lipids. Recently, the use of nanoparticles is turning into a promising option to improve mechanical and barrier properties of biodegradable biopolymer-based films (Abdollahi, Rezaei, & Farzi, 2012).

Among nanoparticles, metal oxides like TiO_2 have evidenced

* Corresponding author.
** Corresponding author.
E-mail addresses: mahdi_ojagh@yahoo.com (S.M. Ojagh), abdollahi.mkh@gmail.com (M. Abdollahi).

http://dx.doi.org/10.1016/j.lwt.2016.03.011
0023-6438/

good potential to improve functional properties (such as anti-radiation and antimicrobial activities) of biodegradable films (Li et al., 2011). With its low price and nontoxic and photostable properties, TiO_2 has gained special attention among proponents of these metal nanoparticles (Feng et al., 2007). In addition, when TiO_2 is incorporated into a biopolymer matrix, it may decrease transmittance in light's visible, UVA and UVB regions (Li et al., 2011). Therefore, TiO_2 might be a good way to prevent spoilage from light-induced oxidation in food packaging systems. However, there is no published study about the combined effect of agar layer and TiO_2 nanoparticle on the properties of fish gelatin-based film.

Thus, the present study aimed to develop a new biodegradable bilayer gelatin/agar film incorporating TiO_2 for food packaging, with minimum water sensitivity and maximum UV light barrier properties. The gelatin/agar films, with or without TiO_2, were characterized using SEM and XRD analysis. Film transparency, surface color, water vapor permeability and mechanical properties of the bilayer films were also examined.

2. Materials and methods

2.1. Materials

Agar–agar (analytical grade) and glycerol were obtained from Merck Co., Germany. Gelatin from cold water fish skin was purchased from Sigma–Aldrich (St. Louis, MO, USA). TiO_2 nanoparticles obtained from TEKCAN Co., Iran were in the anatase and rutile phase, ranging from 10 to 15 nm.

2.2. Preparation of bilayer films

Gelatin/agar bilayer films were prepared by a two-step casting technique. First, the agar layer was produced by solubilization of 1.5 g of agar powder in 100 mL of distilled water heated at 90 °C for 30 min under 600 rpm magnetic stirring. Then, glycerol (as plasticizer) was added at a concentration of 35% (g/100 g of agar powder). The agar film-forming solution was cast onto Petri dishes (8 cm in diameter) and allowed to dry in an oven at 45 °C for 24 h. In the next step, the gelatin film-forming solution (4 g/100 mL) was prepared by hydrating 4 g of the fish gelatin in 100 ml distilled water for 30 min, and then heating it at 55 °C for 30 min under continuous stirring. Glycerol was also added at a concentration of 35% of the total dry basis. Next, the TiO_2 dispersions (in ratios of 0, 0.5, 1 and 2 g/100 g of the gelatin) were added to the gelatin solution and stirring was continued for 1 h. Then, it was sonicated with assistance of a probe ultrasound (S-4000 Ultrasonic Processor, Misonix, Farmingdale, NY, USA) for 30 min, and stirring was subsequently continued for 1 h. Next, the solutions were degassed under vacuum for 15 min to remove air bubbles. Solutions were then cast atop the agar film and dried at 25 °C in the oven for 24 h. Finally, the obtained bilayer film was stored in desiccators containing saturated magnesium nitrate solution at 25 °C and 52.89% relative humidity for 48 h.

2.3. X-ray diffraction (XRD) analysis

Crystallinity of TiO_2 in the gelatin/agar bilayer films was determined by XRD analysis. Film samples were cut into rectangular pieces (3 × 2 cm), mounted on glass supports and used for the analysis. XRD patterns of the films were obtained using a D8 ADVANCE Polycrystal X-ray Diffractometer (Bruker Co., Germany) with a nickel-filtered Cu Kα radiation beam in an angular range of 20–80 (2θ) at a voltage of 40 kV and current of 40 mA.

2.4. Scanning electron microscopy (SEM)

The surface morphology of the gelatin/agar-TiO_2 bilayer films was examined by scanning electronic microscopy using a Philips XL 30 scanning electron microscope with an operating voltage of 20.0 kV (Philips, Eindhoven, the Netherlands). All samples were mounted on metal stubs, sputtered with gold for conductivity and observed at various magnifications.

2.5. Apparent surface color measurement

Film color was determined by a colorimeter (BYK-Gardner, Columbia, MD, USA). The film samples were placed on a standard white plate ($L^* = 94.63$, $a^* = -0.88$ and $b^* = 0.65$). Color parameters such as L (lightness), a (green-red), and b (blue-yellow) values were determined from the average of eight readings from each sample. The total color difference (ΔE) and whiteness index (WI) of the films were determined as follows:

$$\Delta E = \sqrt{(\Delta L^*)^2 + (\Delta a^*)^2 + (\Delta b^*)^2} \quad (1)$$

$$WI = 100 - \sqrt{(100 - L^*)^2 + a^{*2} + b^{*2}} \quad (2)$$

where ΔL, Δa and Δb are the differences between the color of the standard color plate and the film samples.

2.6. Spectrophotometric analyses

Transmission spectra of the bilayer film in the wavelength range of 200–800 nm were measured by a UV–VIS spectrophotometer (Lambda 25, PerkinElmer, Fremont, CA, USA). Each film specimen was cut into rectangles and placed directly in a spectrophotometer test cell, and ambient air was used as reference. Opacity of the bilayer films was evaluated according the method described by Abdollahi, Alboofetileh, Rezaei, and Behrooz (2013). Light absorbance of the bilayer film specimens at 600 nm was used to calculate opacity according the following equation:

$$\text{Opacity} = \frac{\text{Abs } 600}{t} \quad (3)$$

Where Abs600 is a value of absorbance at 600 nm and t is the film thickness (mm). Measurements were performed in at least three replicates.

2.7. Mechanical properties

The mechanical properties of each film sample were measured by analyzing the tensile strength (TS) and elongation at break (EB) according to ASTM standard method D 882-02 (ASTM, 2002) with an Instron Universal Testing Machine (Model A1 700, Gotech, Taiwan). Samples were cut into rectangular strips measuring 2.54 × 10 cm. The initial grip separation was set at 50 mm and crosshead speed at 50 mm/min. Measurements were performed on at least five film specimens.

2.8. Moisture content (MC)

MC of each film sample was measured by drying small specimens of films (2.5 cm × 2.5 cm) in a hot air oven at 105 ± 1 °C for 24 h. Samples were placed on glass Petri dishes that were weighed before and after oven drying. MC values were analyzed in at least triplicate and results were expressed as (g/100 g).

2.9. Calculation of water vapor permeability (WVP)

Water vapor permeability of bilayer films was determined gravimetrically according to ASTM E96- 92 method (ASTM, 2002) as described by Abdollahi et al. (2012). The films were sealed on the top of a glass permeation cell (internal diameter = 3 cm). The cell contained distilled water (100% RH; 2.337×10^3 Pa vapor pressure at 20 °C) placed in a desiccator and maintained at 20 °C and 1.5% RH (28.044 Pa water vapor pressure) with silica gel, and air was stirred in the desiccators. Weight loss of the permeation cell was determined at intervals of 2 h for 10 h. The weight loss of the cell was considered equal with the transferred water through the film and adsorbed by the desiccant. The slope of weight loss vs. time was obtained by linear regression. The WVP was then calculated as follows:

$$WVP = (WVTR \times L)/\Delta P \quad (4)$$

Where WVTR (water vapor transmission rate, $kg/m^2\ s^1$) is the measured slope, L is the mean film thickness (m), and ΔP is the partial water vapor pressure difference (Pa) between the two sides of the film. This test was repeated three times for each specimen to confirm its repeatability.

2.10. Swelling

Swelling ratio (SR) of the bilayer films was evaluated by determining water sorption according to the method explained by Lavorgna, Piscitelli, Mangiacapra, and Buonocore (2010). The film sample (2 cm × 2 cm), desiccated 24 h by silica gel and then the pieces were weighed to determine their dry mass. The weighed samples were placed in closed beakers containing 50 mL of distilled water (pH 7) and stored at 25 °C. The swelling of the samples was evaluated by measuring their weight increment periodically until equilibrium. The films' wet surfaces were gently blotted with a tissue before weighing with a balance accurate to 0.001 g. The procedure was repeated three times for each sample to confirm its repeatability. The water gain of each sample was calculated as follows:

$$\text{Swelling}\ (\%) = (\text{Weight of wet film} - \text{Weight of dry film}) \times 100\ /\ \text{Weight of dry film} \quad (5)$$

2.11. Water solubility (S)

Water solubility of the bilayer films was determined according to the method explained by Tunc et al. (2007). Samples of the films were cut in 2.5 × 2.5 cm rectangles and then dried at 105 °C for 24 h in order to measure their initial dry weight (Wi). After 24 h agitation in 50 mL distilled water at 25 °C, the solutions were filtered through Whatman No. 1 filter paper. Then, the papers were dried in a forced-air oven (105 °C, 24 h) to achieve final dry weight (Wf). The film solubility (%) was calculated using the following equation:

$$\text{Solubility in water}\ (\%) = (Wi - Wf) \times 100\ /\ Wi \quad (6)$$

2.12. Statistical analyses

The statistical analysis of film properties were measured with individually prepared films in triplicate as the replicated experimental, and mean values with standard deviations (SD) were reported. One-way analysis of variance (ANOVA) and Duncan's multiple range tests were used to determine significant differences between factors and levels. Differences with a probability value of <0.05 were considered significant and all data are presented as mean ± SD.

3. Results and discussion

3.1. X-ray diffraction (XRD) of bilayer films

The crystallinity of TiO_2 in the bilayer films was revealed by analysis of the X-ray diffraction patterns, and the results are illustrated in Fig. 1. The anatase and rutile characteristic structure of TiO_2 is such that each has several peaks at 2θ of 26–75° recognized for pure TiO_2 (Kaplan, Erjavec, Dražić, Grdadolnik, & Pintar, 2016), shown by red and blue lines, respectively. According to the Scherrer equation ($D = 0.9\lambda/\beta\cos\theta$, where D is the crystallite size, λ is the wavelength of the X-ray radiation, β is the full width at half maximum, and θ is the angle of diffraction), the average crystallite size of TiO_2 nanoparticles was estimated to be 50–83 nm. The obtained crystallite size coincides with those previously reported by Li et al. (2011) (40–80 nm) and Zolfi, Khodaiyan, Mousavi, and Hashemi (2014) (80 nm) for TiO_2 nanoparticles. Regarding the gelatin/agar bilayer film, when TiO_2 concentration was very low (0.5 g/100 g), the crystalline structure of the nanoparticle was almost undetectable and was X-ray amorphous. When the concentration of TiO_2 in the gelatin layer increased and reached 2 g/100 g, the intensity of the peaks increased, and the obtained pattern was approximately the same as that of pure anatase TiO_2 (Li et al., 2011). Bilayer film containing 2 g/100 g of TiO_2 showed seven distinctive diffraction peaks at 2θ of 26, 37, 48, 55, 63, 70 and 75°, indicating the presence of crystalline anatase TiO_2 in the gelatin film matrix (Li et al., 2011; Zhou, Wang, & Gunasekaran, 2009). As previously suggested by Li et al. (2011), at low TiO_2 concentrations the coverage of protein on the surface of the TiO_2 particles reduces the crystallization characteristics of the nanoparticles, which is not reflectable in the XRD. However, self-assembled large TiO_2 agglomerates formed at high concentration of nanoparticles (2 g/100 g) could recover their crystallization ability.

3.2. Film images and scanning electron microscopy (SEM)

The photographs of (a) gelatin/agar film and (b) gelatin/agar containing 0.5 g/100 g TiO_2, (c) containing 1 g/100 g TiO_2 and (d) containing 2 g/100 g TiO_2 are presented in Fig. 2 to show their

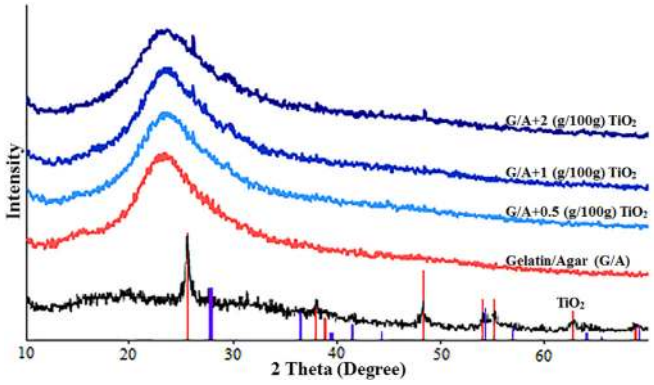

Fig. 1. X-Ray diffraction patterns of TiO2 powder, gelatin/agar film and gelatin/agar films with different percentages of TiO2 nanoparticles. 00-021-1272 (*) – Anatase, syn – TiO_2 – WL: 1.5406. 00-021-1276 (*) – Rutile, syn – TiO_2 – WL: 1.5406.

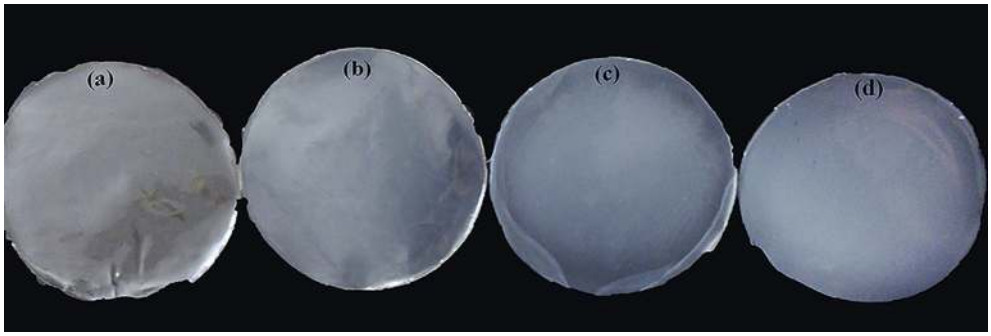

Fig. 2. Photographs of (a) gelatin/agar bilayer film, and gelatin/agar bilayer films (b: 0.5 g/100 g TiO_2; c: 1 g/100 g TiO_2; d: 2 g/100 g TiO_2).

macroscopic appearance. As can be seen, all films had a homogenous and smooth appearance. However, with increasing concentration of TiO_2 nanoparticles in the bilayer films, the films' transparency decreased, so that the bilayer film containing 2 g/100 g TiO_2 looked more translucent and opaque.

Additionally, the surface microstructure of bilayer films was tested with scanning electron microscopy as shown in Fig. 3. As can be seen, the control bilayer film had smooth and homogenous surface microstructures without crack and pores. At low concentration (0.5 and 1 g/100 g), TiO_2 nanoparticles were uniformly distributed on the surface of the bilayer films and small properly dispersed nanoparticles were scarcely visible on the surface. However, the size of particles increased and agglomerates formed after increasing the concentration of TiO_2, especially at 2 g/100 g, which reduced film surface homogeneity as well. This might be due to the high surface energy of the TiO_2 nanoparticles, which caused agglomeration of the nanoparticles at high concentration and prevented their homogenous dispersion in the gelatin matrix. Similarly, Li et al. (2011) and Zolfi et al. (2014) showed a high amount of agglomeration when TiO_2 was added to kefiran-whey protein, or whey protein isolate, respectively, at concentrations higher than 1 g/100 g.

3.3. Film surface color

Film color is of utmost importance, because it has a direct impact on the appearance of a packaged product and may influence the acceptability of product by the consumer. Biodegradable films and nanocomposites are expected to be as near to colorless as possible to simulate the appearance of common polymeric films, which are now used in the food packaging industry (Rhim, Gennadios, Weller, & Hanna, 2002). The parameters of green-red (a^*), blue-yellow (b^*), lightness (L^*), the difference between the color of the white plate and samples (ΔE^*) and the whiteness index (WI^*) values are shown in Table 1. Results showed that ΔE^* and a^* value of the films significantly decreased by adding TiO_2 to the polymer from 3.98 to 2.67 for gelatin/agar films, to 3.01 and 2.08, respectively, for those containing 2 g/100 g TiO_2 ($p < 0.05$). In contrast, the parameters of L^*, b^*, and WI^* increased by adding TiO_2 nanoparticles (Table 1). As shown in the surface photograph of the films, TiO_2 generated more opaque and whiter films, especially at 2 g/100 g, which might be related to the white color of TiO_2 in solution form.

3.4. Light transmittance and film opacity

The results of spectroscopic scanning of gelatin/agar films with and without TiO_2 nanoparticles in the UV and visible light range (200–800 nm) are shown in Fig. 4a. Neat gelatin/agar bilayer film showed very high transmittance (about 90%) in the viable range. However, when the TiO_2 was incorporated into the gelatin layer and its concentration increased, a dramatic decrease was observed in the transmittance values of the bilayer films. TiO_2's characteristics as a metallic nanoparticle with high aspect ratio and crystalline structure may cause this drop in transmittance values. TiO_2 nanoparticles can greatly facilitate diffuse reflection of light on their interface, due to their large specific surface area and high refractive index (Liu, Xiong, Chen, Lin, & Tu, 2015). In addition, the enlarged image of the UV region (200–300 nm) indicated very low transmission of UV light for the films incorporated with TiO_2, especially at 2 g/100 g, when compared to the control bilayer film. This result revealed that TiO_2 nanoparticles tend to absorb UV because short-wave light (UV) has more energy than long-wave light (infrared). In this case, TiO_2 presence can cause photocatalysis to occur by absorbing more ultraviolet light. These results coincide with those previously reported about the addition of TiO_2 nanoparticles to WPI (Li et al., 2011), WPI/kefiran (Zolfi et al., 2014) and high amylase starch (Liu et al., 2015). Since UV light more intensively and easily causes lipid oxidation and food deterioration, this ability of TiO_2 nanoparticles to absorb ultraviolet and visible light has great potential application in delaying lipid oxidation in light-sensitive food products, such as packaging material.

The opacity of a material is an indication of how much light passes through it (Casariego et al., 2009); therefore, it is an established measurement of the transparency of a film. Fig. 4b exhibits the opacity values of bilayer films with different percentages of TiO_2 nanoparticles. The opacity of gelatin/agar film (control) was low (7.15), disclosing its high transparency. However, opacity value increased slightly by the incorporation of nano-TiO_2 content up to 1 g/100 g (11.2), whereas more TiO_2 (2 g/100 g) significantly increased the opacity of the bilayer film ($p < 0.05$) up to 17.89. These results agree with those of Zhou et al. (2009) and Zolfi et al. (2014), who incorporated TiO_2 nanoparticles into both whey protein and kefiran-whey protein film. In general, reinforcing elements with diameters of less than one-tenth of visible light wavelengths are not expected to cause light scattering (Siró & Plackett, 2010). Thus, the slight increase in film opacity at low TiO_2 concentrations can be related to the nanoparticles' absorptive or reflective properties, as shown in spectroscopic scanning of the films. However, the dramatic increase in opacity at 2 g/100 g might also result from the partial agglomeration and self-networking of the nanoparticles within the gelatin matrix, which hinder light passage through the bilayer film (Zolfi et al., 2014). High amounts of agglomeration were also shown in the SEM of bilayer films containing 2 g/100 g TiO_2, which can intensify light abstraction in the film matrix.

3.5. Mechanical properties of the films

Table 2 displays mechanical properties, which consist of tensile strength (TS) and elongation at break (EB) of the gelatin/agar

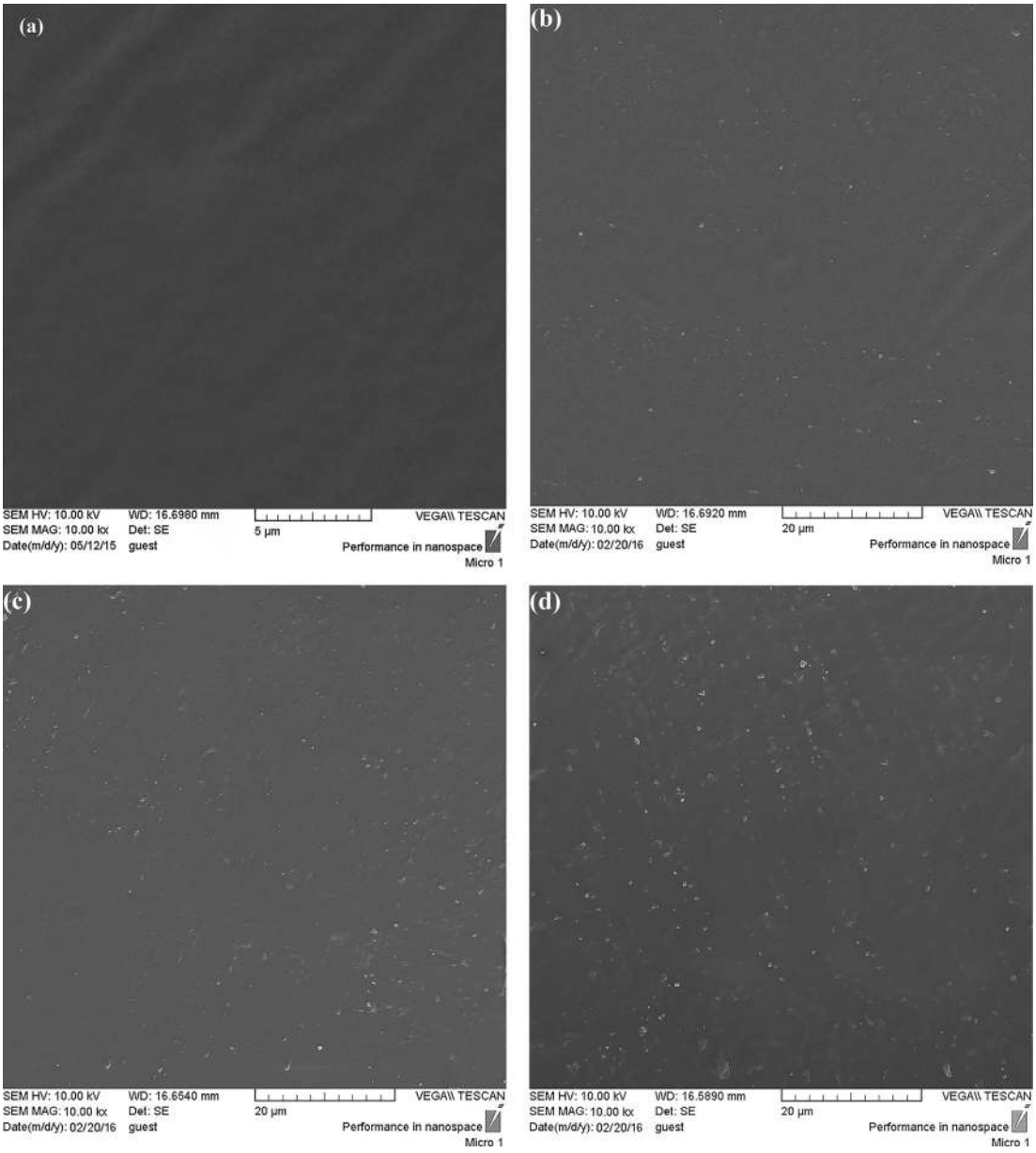

Fig. 3. SEM micrographs of the surface of (a) gelatin/agar (control), (b) gelatin/agar +0.5 g/100 g TiO_2 (c) gelatin/agar +1 g/100 g TiO_2, gelatin/agar +2 g/100 g TiO_2, bilayer films.

Table 1
Surface color parameters of gelatin/agar bilayer films.

Film sample	L^*	a^*	b^*	ΔE	WI
Gelatin/agar	93.11 ± 0.20^{c}	2.67 ± 0.05^{a}	-0.3 ± 0.11^{c}	3.98 ± 0.06^{a}	92.60 ± 0.17^{d}
Gelatin/agar-0.5 (g/100 g) TiO_2	94.41 ± 0.10^{b}	2.46 ± 0.05^{ab}	0.03 ± 0.11^{b}	3.41 ± 0.07^{b}	93.89 ± 0.11^{c}
Gelatin/agar-1 (g/100 g) TiO_2	94.77 ± 0.16^{a}	2.32 ± 0.18^{b}	0.13 ± 0.05^{b}	3.25 ± 0.19^{bc}	94.27 ± 0.11^{b}
Gelatin/agar-2 (g/100 g) TiO_2	95.08 ± 0.22^{a}	2.08 ± 0.15^{c}	$0.4 \pm .0.00^{a}$	3.01 ± 0.14^{c}	94.64 ± 0.22^{a}

Same superscript letter in the same column indicate that they are not statistically different ($p < 0.05$).

bilayer films incorporated with TiO_2 nanoparticles at different concentrations. Film thickness was not significantly affected ($p > 0.05$) by the addition of TiO_2 nanoparticles. This may be due to the small diameter of these nanoparticles. Upon increasing the concentration of nanoparticles' TiO_2 to 0.5 g/100 g, the TS value of the bilayer films increased from 10.80 to 13.91 MPa; however, the TS decreased again with further increase of the filler content up to 2 g/100 g TiO_2. However, the addition of TiO_2 from 0.5 g/100 g–2 g/100 g concentration significantly reduced the EB value of the bilayer films from 48.17 to 37.47% for the gelatin/agar bilayer films ($p < 0.05$). The improvement observed in the TS of the bilayer gelatin/agar films by increasing the filler content up to 0.5 g/100 g may be related to the reinforcement effect of homogeneously dispersed high-strength metal nanoparticles in the biopolymer

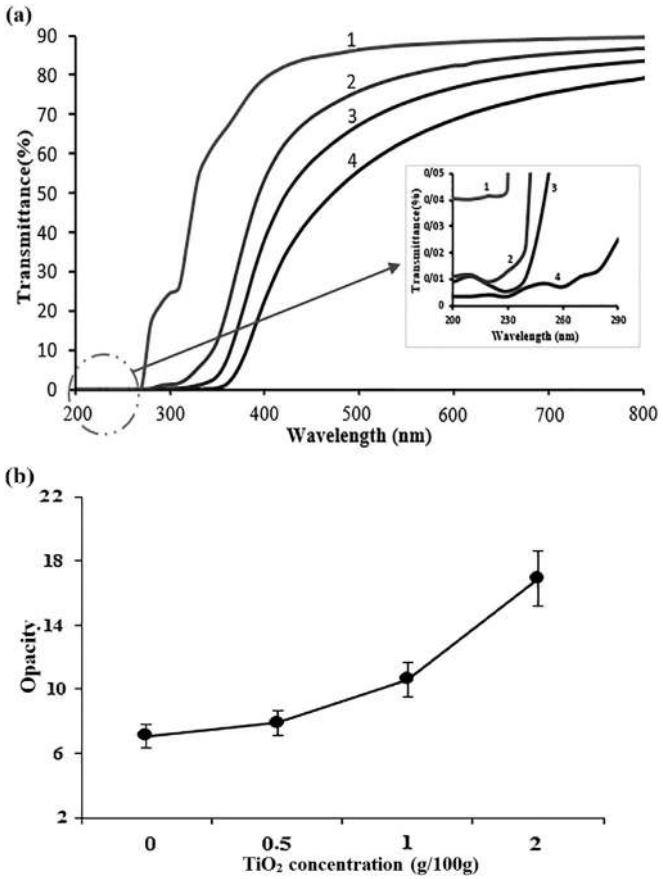

Fig. 4. Effect of TiO_2 content on (a) transmittance and (b) opacity of gelatin/agar bilayer films. (1: gelatin/agar bilayer film, 2: 0.5 g/100 g TiO_2; 3: 1 g/100 g TiO_2; 4: 2 g/100 g TiO_2).

likely be improved by changing the type or concentration of the plasticizer (McHugh & Krochta, 1994).

3.6. Moisture content and water solubility

Table 2 displays the moisture content and water solubility (WS) determine for the gelatin/agar bilayer films with different percentages of nanoparticles. The control gelatin/agar film showed lower MC compared to that of the gelatin/agar containing the nanoparticles. This may result from the hydrophilic nature of the TiO_2 nanoparticles, as reported by Hao, Wang, and Weng (2008).

WS is also considered an important characteristic of biodegradable films for application in food packaging applications, especially when water activity is high or when the film must be in contact with water and act as a food protective (Abdollahi et al., 2013). Neat bilayer gelatin/agar films displayed low WS (29.78%), considerably lower than the solubility of monolayer gelatin film (51.47%) (data not shown). This low WS might be related to the presence of agar, which has low WS at ambient temperature. However, no regular variation of water solubility was observed among the samples. Similarly, Li et al. (2011) reported that adding up to 2 g/100 g TiO_2 did not affect the water solubility of whey protein isolate films. However, Feng et al. (2007) reported that the WS of monolayer silk fibroin in water decreased by adding up to 2 g/100 g nano-TiO_2 particles to the film but an excessive content of nano-TiO_2 particles tended to increase the films' WS.

3.7. Water vapor permeability

WVP is one of the most important functional properties of a food storage film (Jang, Lim, & Song, 2010). Low WVP films reduce moisture transfer between the surrounding atmosphere and the food environment, a primary function of food packaging (Gontard, Guilbert, & Cuq, 1992). The WVP values of the gelatin/agar bilayer

Table 2
Thickness, mechanical properties, film solubility and moisture content of the bilayer films.

Film sample	Thickness (μm)	TS (MPa)	EB (%)	MC (g/100 g)	S (%)
Gelatin/agar	93.27 ± 0.67^{a}	10.80 ± 0.46^{c}	48.17 ± 1.75^{a}	13.90 ± 0.43^{b}	29.78 ± 0.99^{a}
Gelatin/agar-0.5 (g/100 g) TiO_2	93.60 ± 0.10^{a}	13.91 ± 1.39^{a}	40.86 ± 1.59^{b}	14.83 ± 0.29^{a}	30.11 ± 0.46^{a}
Gelatin/agar-1 (g/100 g) TiO_2	93.78 ± 0.77^{a}	12.71 ± 0.95^{ab}	38.53 ± 2.63^{b}	14.90 ± 0.13^{a}	29.76 ± 0.51^{a}
Gelatin/agar-2 (g/100 g) TiO_2	93.92 ± 0.33^{a}	11.12 ± 0.09^{bc}	37.47 ± 0.83^{b}	15.25 ± 0.10^{a}	31.10 ± 0.73^{a}

Different letters in the same column (a, b, c, d) indicate significant differences among samples ($p < 0.05$). TS: tensile strength, EB: elongation at break, MC: Moisture content, S: solubility.

matrix. It might also be related to the interactions between carboxylic and sulphydryl groups from certain amino acids in the gelatin structure with TiO2 nanoparticles (Zhou et al., 2009). The reduction observed in TS at high TiO_2 content might arise from the possible agglomeration and nonhomogeneous dispersion of nanoparticles at high levels due to the nanoparticles' self-networking, which could reduce both the TS of the nanocomposite, as reported by others, by adding TiO_2 to WPI (Zolfi et al., 2014) and the TS of the silk fibroin (Feng et al., 2007). These results coincide with the high nanoparticle agglomeration observed in the SEM photographs (Fig. 3). In the present study, EB value also declined with increasing TiO2 concentration. This fact might be related to the rigid nature of the filler, which restricts the motion of the gelatin matrix in terms of the strong interactions between the fillers and biopolymer matrix which caused the antiplasticizing effect of TiO_2 nanoparticles in gelatin/agar matrix (Li et al., 2011). Consequently, the mechanical properties of the bilayer film would

films containing TiO_2 nanoparticles are shown in Fig. 5a. The WVP of the control gelatin/agar film was 3.26×10^{-10} g/m^2 s Pa, which decreased notably (about 30%) when 0.5 g/100 g TiO_2 was added to the gelatin layer. However, when more than 0.5 g/100 g was added to the biopolymeric matrix, the WVP values gradually declined to 2.22×10^{-10} g/m^2 s Pa, which was significantly lower than observed in the control bilayer film ($p < 0.05$). Generally, the water vapor barrier properties of composites are improved if the filler is less permeable, less hydrophilic and has good dispersion in the matrix and a high aspect ratio (Pereda, Amica, Rácz, & Marcovich, 2011). This phenomenon of WVP reduction in the presence of nanoparticles could related mostly to the tortuous path introduced by impermeable TiO_2 distributed in the matrix. They increase pass length for water molecules by forcing the permeating molecules to wiggle around them in a random walk (Chang, Jian, Zheng, Yu, & Ma, 2010; Pereda et al., 2011). At low levels, the TiO_2 nanoparticles could disperse properly in the gelatin matrix (as shown by

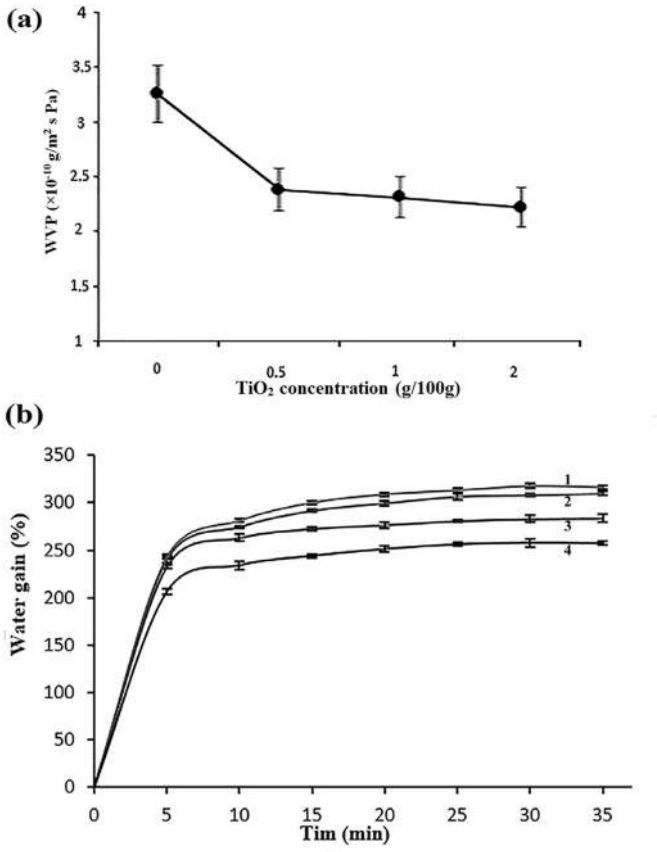

Fig. 5. Effect of TiO_2 content on (a) water vapor permeability (WVP) and (b) water sorption profile of gelatin/agar bilayer films. (1: gelatin/agar bilayer film, 2: 0.5 g/100 g TiO_2; 3: 1 g/100 g TiO_2; 4: 2 g/100 g TiO_2).

SEM in Fig. 3), which blocks the water vapor. However, at higher concentration due to high surface energy the excessive TiO_2 was easily agglomerated (as shown by SEM), which actually decreased the effective content of the nanoparticles and facilitated the water vapor permeation (Chang et al. 2010). These results also coincide with those previously reported by Li et al. (2011) regarding the incorporation of TiO_2 nanoparticles into WPI films.

3.8. Swelling

The swelling behavior of gelatin/agar films in aqueous solution is shown in Fig. 5b. The results indicated that all bilayer films could be stable during a 35 min evaluation and absorbed water quickly during 5 initial min of soaking. After 10 min of soaking, equilibrium water uptake was reached. The neat bilayer agar/gelatin film absorbed more than 200% water, and it reached 250% and 300% for samples containing 0.5 and 1 g/100 g TiO_2. However, it did not increase considerably by increasing TiO_2 content to 2 g/100 g. In other words, the swelling ratio of bilayer films rose by increasing TiO_2 content from 0.5 to 1 in the bilayer films. This might be due to the hydrophilic nature of the TiO_2 nanoparticles as showed by Hao et al. (2008). They also reported that increasing the size of nanoparticles reduced their hydrophilic property and increased their hydrophobicity. As shown in the SEM photographs (Fig. 3), TiO_2 nanoparticles size increased due to agglomeration with an increase in the nanoparticles' concentration in the gelatin matrix. This might reduce the hydrophilic property of TiO2 and might explain the similarities observed in SR between bilayer films containing 1 g/100 g and 2 g/100 g TiO_2.

4. Conclusions

Bilayer gelatin/agar nanocomposite films were developed by adding TiO_2 nanoparticles at various concentrations (0.5, 1 and 2 g/100 g) to the upper layer (gelatin) using the solution casting method. Results demonstrated that some properties of the bilayer films were greatly influenced by TiO_2 nanoparticle content. Adding TiO_2 nanoparticles to the gelatin layer affected light transmission, such that the films containing 0.5–2 g/100 g TiO_2 considerably prevented the transmission of UV light through the gelatin/agar films. Adding 0.5 g/100 g TiO_2 to the gelatin/agar bilayer films improved the water vapor barrier and mechanical strength of the bilayer films. Thus, results suggest that the bilayer films containing nano-TiO_2 at low concentrations may have potential for preservation of light-sensitive food. However, future studies on real food systems are required.

Acknowledgments

The authors wish to thank Sunny Skies for the English editing.

References

Abdollahi, M., Alboofetileh, M., Rezaei, M., & Behrooz, R. (2013). Comparing physico-mechanical and thermal properties of alginate nanocomposite films reinforced with organic and/or inorganic nanofillers. *Food Hydrocolloids, 32*(2), 416–424.
Abdollahi, M., Rezaei, M., & Farzi, G. (2012). A novel active bionanocomposite film incorporating rosemary essential oil and nanoclay into chitosan. *Journal of Food Engineering, 111*, 343–350.
ASTM. (2002). *Standard test methods for tensile properties of plastics. Method ASTM D882–02. Philadelphia, PA*. American Society for Testing and Materials.
Casariego, A., Souza, B., Cerqueira, M., Teixeira, J., Cruz, L., Díaz, R., et al. (2009). Chitosan/clay films' properties as affected by biopolymer and clay micro/nanoparticles' concentrations. *Food Hydrocolloids, 23*(7), 1895–1902.
Chang, P. R., Jian, R., Zheng, P., Yu, J., & Ma, X. (2010). Preparation and properties of glycerol plasticized-starch (GPS)/cellulose nanoparticle (CN) composites. *Carbohydrate Polymers, 79*(2), 301–305.
Farris, S., Schaich, K. M., Liu, L. S., Cooke, P. H., Piergiovanni, L., & Yam, K. L. (2011). Gelatin-pectin composite films from polyion-complex hydrogels. *Food Hydrocolloids, 25*, 61–70.
Feng, X. X., Zhang, L. L., Chen, J. Y., Guo, Y. H., Zhang, H. P., & Jia, C. I. (2007). Preparation and characterization of novel nanocomposite films formed from silk fibroin and nano-TiO_2. *International Journal of Biological Macromolecules, 40*(2), 105–111.
Freile-Pelegrín, Y., Mader-Santana, T., Robledo, D., Veleva, L., Quintana, P., & Azamar, J. A. (2007). Degradation of agar films in a humid tropical climate: thermal, mechanical, morphological and structural changes. *Polymer Degradation and Stability, 92*, 244–252.
Gontard, N., Guilbert, S., & Cuq, J.-L. (1992). Edible wheat gluten films-influence of the main process and environmental-conditions on thermal, mechanical and barrier properties. *Abstracts of Papers of the American Chemical Society, 204*, 217–AGFD.
Hao, Y. Q., Wang, Y. F., & Weng, Y. X. (2008). Particle-size-dependent hydrophilicity of TiO_2 nanoparticles characterized by Marcus reorganization energy of interfacial charge recombination. *The Journal of Physical Chemistry C, 112*(24), 8995–9000.
Jang, S.-A., Lim, G.-O., & Song, K. B. (2010). Original article: use of nano-clay (Cloisite Na+) improves tensile strength and vapour permeability in agar rich red algae (Gelidium corneum)–gelatin composite films. *International Journal of Food Science & Technology, 45*(9), 1883–1888.
Kanmani, P., & Rhim, J. W. (2014). Physical, mechanical and antimicrobial properties of gelatin based active nanocomposite films containing AgNPs and nanoclay. *Food Hydrocolloids, 35*, 644–652.
Kaplan, R., Erjavec, B., Dražić, G., Grdadolnik, J., & Pintar, A. (2016). Simple synthesis of anatase/rutile/brookite TiO_2 nanocomposite with superior mineralization potential for photocatalytic degradation of water pollutants. *Applied Catalysis B: Environmental, 181*, 465–474.
Kim, S. K., & Mendis, E. (2006a). Bioactive compounds from marine processing by products – a review. *Food Research International, 39*, 383–393.
Kim, S. K., & Mendis, E. (2006b). Bioactive compounds from marine processing by products – a review. *Food Research International, 39*, 383–393.
Lavorgna, M., Piscitelli, F., Mangiacapra, P., & Buonocore, G. G. (2010). Study of the combined effect of both clay and glycerol plasticizer on the properties of chitosan films. *Carbohydrate Polymers, 82*(2), 291–298.
Li, Y., Jiang, Y., Liu, F., Ren, F., Zhao, G., & Leng, X. (2011). Fabrication and characterization of TiO_2/whey protein isolate nanocomposite film. *Food Hydrocolloids, 25*(5), 1098–1104.
Liu, C., Xiong, H., Chen, X., Lin, S., & Tu, Y. (2015). Effects of nano-TiO_2 on the

performance of high-amylose starch based antibacterial films. *Journal of Applied Polymer Science, 132*(32).
Martucci, J. F., & Ruseckaite, R. A. (2009). Tensile properties, barrier properties and biodegradation in soil of compression-molded gelatin-dialdehyde starch films. *Journal of Applied Polymer Science, 112*(4), 2166–2178.
McHugh, T. H., & Krochta, J. M. (1994). Sorbitol-plasticized vs glycerol-plasticized whey protein edible films-integrated oxygen permeability and tensile property evaluation. *Journal of Agricultural and Food Chemistry, 42*(4), 841–845.
Pavlath, A. E., Gosset, C., Camirand, W., & Roberton, G. H. (1999). Ionomeric films of alginic acid. *Journal of Food Science, 64*(1), 61–63.
Pereda, M., Amica, G., Rácz, I., & Marcovich, N. E. (2011). Structure and properties of nanocomposite films based on sodium caseinate and nanocellulose fibers. *Journal of Food Engineering, 103*(1), 76–83.
Ramos, Ó. L., Reinas, I., Silva, S. I., Fernandes, J. C., Cerqueira, M. A., Pereira, R. N., et al. (2013). Effect of whey protein purity and glycerol content upon physical properties of edible films manufactured therefrom. *Food Hydrocolloids, 30*(1), 110–122.
Rhim, J. W., Gennadios, A., Weller, C. L., & Hanna, M. A. (2002). Sodium dodecyl sulfate treatment improves properties of cast films from soy protein isolate. *Industrial Crops and Products, 15*(3), 199–205.
Rhim, J. W., & Wang, L. F. (2013). Mechanical and water barrier properties of agar/κ-carrageenan/konjac glucomannan ternary blend biohydrogel films. *Carbohydrate Polymers, 96*(1), 71–81.
Siró, I., & Plackett, D. (2010). Microfibrillated cellulose and new nanocomposite materials: a review. *Cellulose, 17*(3), 459–494.
Tunc, S., Angellier, H., Cahyana, Y., Chalier, P., Gontard, N., & Gastaldi, E. (2007). Functional properties of wheat gluten/montmorillonite nanocomposite films processed by casting. *Journal of Membrane Science, 289*(1), 159–168.
Weber, C., Haugaard, V., Festersen, R., & Bertelsen, G. (2002). Production and applications of biobased packaging materials for the food industry. *Food Additives & Contaminants, 19*(S1), 172–177.
Yakimets, I., Wellner, N., Smith, A. C., Wilson, R. H., Farhat, I., & Mitchell, J. (2005). Mechanical properties with respect to water content of gelatin films in glassy state. *Polymer, 46*(26), 12577–12585.
Zhou, J., Wang, S., & Gunasekaran, S. (2009). Preparation and characterization of whey protein film incorporated with TiO_2 nanoparticles. *Journal of Food Science, 74*(7), N50–N56.
Zolfi, M., Khodaiyan, F., Mousavi, M., & Hashemi, M. (2014). The improvement of characteristics of biodegradable films made from kefiran–whey protein by nanoparticle incorporation. *Carbohydrate Polymers, 109*, 118–125.